RSC Advances

Phase stability, hardness and bond characteristic of ruthenium borides from first-principles

Y. Pan [1,2] *, W.T. Zheng[2], K. Xu[1], X.M. Luo[1], W. Li[1], Y.C. Yang[1]

[1] State Key Laboratory of Advanced Technologies for Comprehensive Utilization of Platinum Metals, Kunming 650106, PR China.

[2] Department of Materials Science, Key Laboratory of Automobile Materials of MOE and State Key Laboratory of Superhard Materials, Jilin University, Changchun 130012, PR China

* *E-mail address*: y_pan@ipm.com.cn (Y. Pan).

The structural stability, elastic modulus, hardness and electronic structure of RuB_{2-x} ($0 \le x \le 2$) are systematically investigated by using first-principles approach. The calculated results indicate that the boron-poor region is more stable than boron-rich region. The Ru_2B_3 has high bulk modulus, high shear modulus and high Young′s modulus compared with the RuB_2 and RuB. Moreover, the calculated intrinsic hardness of Ru_2B_3 with hexagonal structure (Space group: *P63/mmc*) is 49.2 GPa, which is a potential superhard material. The high hardness of Ru_2B_3 originates from the feature of triangular pyramid bonds, which is composed of B-B covalent bond as base and Ru-B covalent bonds as two sides. The B-B and Ru-B covalent bonds in *a*-*c* plane resist the applied load, which is origin of high elastic modulus and hardness.

1. Introduction

In recent years, the transition metal borides (TMBs) have received considerable attention due to the high bulk modulus, high hardness, ultra-incompressible, good thermal stability and a degree of metallic behavior *etc*[1-6]. For examples, the average hardness of ReB_2, WB_4 and $Os_{0.5}W_{0.5}B_2$ is about of 48 GPa, 46.2 GPa and 40.4 GPa, respectively[7, 8]. However, numerous TMBs are not superhard materials. Therefore, exploring novel TMBs superhard materials is necessary.

For Ru-based borides, although the calculated bulk modulus of RuB_2 is about of 334.8 GPa[9], the average hardness of RuB_2 rapidly decreased from 24.4 GPa to 14.4 GPa with increasing the applied load[10, 11]. The calculated intrinsic hardness of RuB_2 is 36.1 GPa, which is lower than 40 GPa[12]. Moreover, our previous research result shows that the average measured hardness of $RuB_{1.1}$ is only about of 10.6 GPa, and the calculated bulk modulus is 346 GPa[13]. Therefore, these results suggest that Ru-based borides are not superhard materials. In 2009, Rau *etc* experimental reported that the biphasic ruthenium boride film is 49 GPa, which may be a potential superhard material[14]. They pointed out that the high hardness originates from the microstructure which is composed of two Ru-based boride phases: Ru_2B_3 (main phase) and RuB_2 (second phase). However, the structural, elastic modulus, hardness and electronic structure of only RuB_2 are studied in detail. Unfortunately, the reports of other Ru-based borides (Ru_2B_3, RuB and Ru_8B_{11} *etc*) are scarce.

On the other hand, numerous theoretical calculations show that the high hardness of

TMBs is derived from bond covalency. In fact, the hardness is related not only to the bond covalency but also to other factors such as bond orientation, and the arrangement of bond *etc*. To reveal the hard nature and to search for novel superhard materials, in this paper, the structural stability, elastic modulus, intrinsic hardness and electronic structure of RuB_{2-x} ($0 \le x \le 2$) borides are systematically investigated by first-principles approach. Finally, we predict that the calculated intrinsic hardness of Ru_2B_3 with hexagonal structure is 49.2 GPa, which is a potential superhard material.

2. Computational detail

As we know, RuB_2 has an orthorhombic structure (space group: *Pmmn*, No: 59) with lattice parameters: a= 4.645 Å, b= 2.865 Å and c= 4.045 Å[15]. The Ru and B atoms occupy the 2a (0.0114, 0.2500, 0.8773) and 4f (0.1489, 0.0776, 0.3940) sites (see Fig.1), respectively. To reveal the correlation between hardness and boron concentration, in this paper, we began with a supercell of Ru_8B_{16} representing the host RuB_2. The case of x= 0, 0.125, 0.25, 0.50, 0.75, 1.00, 1.25, 1.50. 1.75 and 2.00, respectively. The main purpose of this work is expected to understand of the relationship between structural stability and hardness for Ru-based borides and stimulate future experimental study.

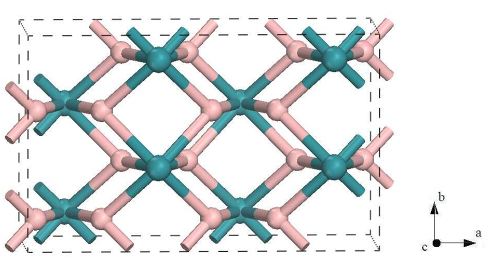

Fig. 1 The model of RuB_2, The blue and orange spheres represent Ru and B atoms, respectively.

All calculations were performed using the CASTEP code[16]. The exchange correlation functional was treated by the generalized gradient approximation (GGA)[17] with Perdew-Burke-Ernzerhof-functionals (PBE)[18], we proved that these ruthenium borides have no spin polarized. The electron-ion interaction was described through the ultrasoft pseudopotentials. A plane-wave basis set for electron wave function with cut-off energy of 360 eV was used. Integrations in the Brillouin zone were performed using special k- point generated with 6×17×12 for these structures. During the structural optimization, no symmetry and no restriction were constrained for unit-cell shape, volume and atomic position. The structural relaxation was stopped until the total energy, the max force and the max displacement were less than 1×10^{-5} eV/atom, 0.001 eV/Å, and 0.001 Å, respectively. In addition, the actual spacing of DOS calculation was less than 0.015 $Å^{-1}$.

3. Results and discussion

To estimate the structural stable each B concentration, the short-range order structure should be considered as large as possible and the total energy of all configurations be calculated and discussed. According to the symmetrical operation, all 55 distinct RuB_{2-x} configurations are designed, corresponding to x= 0, 0.125, 0.25, 0.50, 0.75, 1.00, 1.25, 1.50, 1.75 and 2, respectively.

The formation energies with respect to RuB_{2-x} are calculated by:

$$\Delta E(x) = E(RuB_{2-x}) - [E(Ru) + (2-x)E(B)] \quad (1)$$

Where $E(RuB_{2-x})$, E(Ru) and E(B) are the first-principles calculated total energies of RuB_{2-x} borides, Ru with hexagonal structure and pure B with B_{12} structure, respectively.

Fig. 2 shows the calculated formation energy of RuB_{2-x} as a function of boron concentration. For each boron concentration, the most stable structure is obtained by first-principles calculation. As seen in Fig. 2, the calculated formation energies of RuB_{2-x} are negative, indicating that these borides are stable at ground state. Moreover, the calculated formation energies of Ru, RuB and Ru_2B_3 are lower than RuB_2 by 1.62 eV/atom, 0.37 eV/atom and 0.15 eV/atom, respectively. That is to say, the boron-poor region is more stable than that of boron-rich region. In addition, we note that there is a convex hull x= 0.25. This convex suggest the existence of ordered metastable structure in this Ru-based borides.

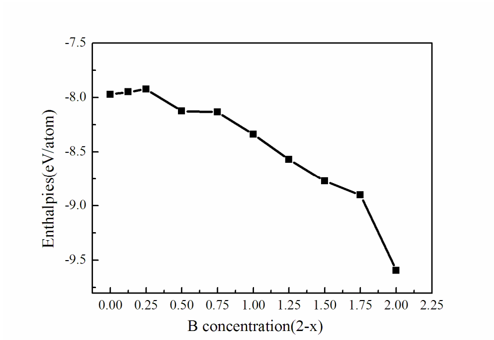

Fig. 2 Calculated formation energy of RuB_{2-x} as a function of boron concentration, x= 0, 0.125, 0.25, 0.50, 0.75, 1.00, 1.25, 1.50, 1.75 and 2.00, respectively.

Elastic constants, bulk modulus, shear modulus, Young′s modulus and Poisson′s ratio are essential for understanding the mechanical properties of a solid. The calculated elastic constants of RuB_2, RuB (x= 1) and Ru_2B_3 (x= 0.5) are listed in Table 1. It is obvious that the elastic constants of these Ru-based borides satisfy the Born stability criteria, indicating that they are mechanically stable at ground state. On the other hand, the calculated elastic constants of RuB_2 are in good agreement with the previous theoretical results. Unfortunately, there are no either experimental data or theoretical studies available on elastic modulus for RuB and Ru_2B_3. Therefore, we hope that the obtained results of RuB and Ru_2B_3 in this work may give useful information for further experimental and theoretical studies.

The elastic constants: C_{11}, C_{22} and C_{33} measure the *a*-, *b*- and *c*- direction resistance to linear compression, respectively. The larger values of C_{11}, C_{22} and C_{33}, the higher the resistance to deformation along corresponding direction. From Table 1, the calculated C_{33} of Ru-based borides are bigger than C_{11} and C_{22}, implying that the resistance to deformation of Ru-based borides along the *c*- direction is stronger than the *a*- direction and *b*- direction, implying that the origin of *c*- direction incompressibility is related not only to the strong B-B and Ru-B covalent bonds but also to the bond orientation (the discussion will be given in the following).

Moreover, the calculated C_{11} of Ru_2B_3 is close to the RuB_2. However, the C_{22} and C_{33} of RuB and Ru_2B_3 are bigger than RuB_2. These results indicate that the RuB and Ru_2B_3 have high resistance to shear deformation along the *b*- direction and *c*- direction. This discrepancy is due to the fact that the structural type of RuB and Ru_2B_3 is different from the RuB_2. For hexagonal structure such as Ru_2B_3, the atomic arrangement along the *b*- direction results in

Table 1 The calculated elastic constants C_{ij} (in GPa) of RuB_2, RuB and Ru_2B_3, respectively.

Type	Method	C_{11}	C_{12}	C_{13}	C_{22}	C_{23}	C_{33}	C_{44}	C_{55}	C_{66}
RuB_2	GGA	518	188	146	458	125	706	118	230	176
	Theo[19]	540	174	154	484	120	719	116	225	183
RuB	GGA	541	187	171	541	171	774	168	168	178
Ru_2B_3	GGA	516	228	222	516	222	831	257	257	114

Table 2 The calculated bulk modulus B (in GPa), shear modulus G (in GPa), Young′s modulus E (in GPa) and Poisson′s ratio δ of RuB_2, RuB and Ru_2B_3, respectively.

Type	Method	B_V	G_V	B_R	G_R	B	G	E	δ
RuB_2	GGA	289	186	284	172	286	179	444	0.241
	Theo[19]	293	191	288	177	290	184		
RuB	GGA	324	191	317	185	321	188	472	0.255
Ru_2B_3	GGA	355	210	342	193	349	202	508	0.257

strong hybridization between B and B atoms, and forms strong B-B covalent bonds, which compensates the weak Ru-B covalent bonds. For orthorhombic structure RuB_2, the Ru-B and B-B covalent bond in *a-c* plane is just the load direction. Therefore, the Ru-B bonds play an important role in measured hardness. Moreover, the calculated C_{33} of Ru_2B_3 is bigger than that of RuB_2 and RuB by 125 GPa and 57 GPa, and the calculated C_{44} for former is bigger than the latter by 139 GPa and 89 GPa, respectively, meaning that the Ru_2B_3 has bigger elastic modulus and high hardness.

To estimate elastic modulus, the Voigt-Reuss-Hill approximation is used in this paper[20]. Table 2 shows the calculated bulk modulus, shear modulus, Young′s modulus and Poisson′s ratio of RuB_2, RuB and Ru_2B_3. We found that the calculated bulk and shear modulus of RuB_2 are in good agreement with the previous theoretical results. Moreover, the bulk and shear modulus of Ru_2B_3 are bigger than that of RuB and RuB_2 and the bulk and shear modulus of RuB are bigger than that of RuB_2. These results suggest that the boron-poor region may have high resistance to shape and shear deformation compared with the boron-rich region. Obviously, it is different from the previous theoretical prediction, which the hardness of boron-rich TMBs is higher than boron-poor TMBs because the boron-rich has more covalent bonds. Therefore, we suggest that the hardness of TMBs is related not only to the bond covalency but also to the other factors such as the bond arrangement. This feature is very demonstrated by the overlap population and bond characteristic (see Table 3 and Fig. 3). In addition, the Young′s modulus is calculated to be in a sequence of Ru_2B_3>RuB> RuB_2. The high Young′s modulus of Ru_2B_3 shows a rather smaller stiffness.

Due to the high bulk and shear modulus, the Ru_2B_3 is expected to be the harder material compared with other Ru-based borides. Here, the calculated intrinsic hardness of Ru-based borides is used by Gao *etc* hard model[21]. The calculated intrinsic hardness, bond length, bond volume and Mulliken overlap population of RuB_2, RuB and Ru_2B_3 are presented in Table 3. It can be seen that the calculated intrinsic hardness of RuB_2 is 36.8 GPa, which is in good agreement with the previous theoretical data (36.1 GPa)[12]. It is worth to notice that the intrinsic hardness of Ru_2B_3 is about of 49.2 GPa. It is very close to the average measure hardness of ruthenium boride film (49 GPa). Therefore, we predict that the Ru_2B_3 is a potential superhard material.

To reveal the origin of high hardness of Ru-based borides, here, the bond characteristic and electronic structure of these Ru-based borides are studied in detail. As shown in Table 3, the calculated bond lengths of B-B and Ru-B covalent bonds of these Ru-based borides are in good agreement with the previous theoretical results. However, the bond lengths of B-B and Ru-B covalent bonds of Ru_2B_3 are shorter than corresponding to the RuB_2 and RuB, respectively. On the other hand, we know that the positive and negative values of overlap population indicate bonding and antibonding state. Obviously, the

Table 3 The calculated bond length d^{μ} (in Å), Mulliken overlap population P^{μ}, bond volume of μ type v^{μ} (in $Å^3$) and intrinsic hardness H_{vcal} (in GPa) of RuB_2, RuB and Ru_2B_3, respectively.

Type	Bond	d^{μ}	P^{μ}	v^{μ}	H_{vcal}	H_{vexp}
RuB_2	B-B	1.817	0.64	1.841		10.9-28.9[22]
	B-B	1.880	1.29	2.040		
	Ru-B	2.190	0.35	3.224	36.8	
RuB	Ru-B	2.173	0.25	3.345	24.7	
Ru_2B_3	B-B	1.804	2.08	1.929		
	Ru-B	2.175	0.88	3.381	49.2	
	Ru-B	2.187	0.52	3.437		
	B-B[22]	1.840				
	Ru-B[23]	2.190				

calculate overlap population of bonds such as B-B and Ru-B covalent bonds of Ru_2B_3 are larger than that of RuB_2 and RuB. These results imply that the local hybridization between Ru and B atoms of Ru_2B_3 is stronger than that of RuB_2 and RuB, and forms the strong B-B and Ru-B covalent bonds. It is very demonstrated by the calculated bond strength (see Table 3).

The bond arrangement also plays an important role in intrinsic hardness. To understand the bond arrangement of RuB_{2-x} borides, the charge densities of chemical bond of RuB_2, RuB and Ru_2B_3 are discussed here. Fig. 3 shows the valence electron density along the RuB_2 (110), RuB (110) and Ru_2B_3 (010) plane, where the critical feature are labeled. Similar to other TMBs, covalent bonding can be observed, and the strong and directional Ru-B covalent bonds are formed in these Ru-based borides. Note that the charge transition between Ru and B atoms of Ru_2B_3 (0.63) is bigger than that of RuB_2 (0.51) and RuB (0.28), indicating that the local hybridization for former is stronger than the latter.

For RuB_2, the network bonds are composed of Ru-B covalent bond with zigzag covalent chains, and directional B-B covalent bond along the *b*- direction, respectively. The Ru-B covalent bonds as two dimensions are formed in the *a*-*c* plane. Therefore, the shear fracture of RuB_2

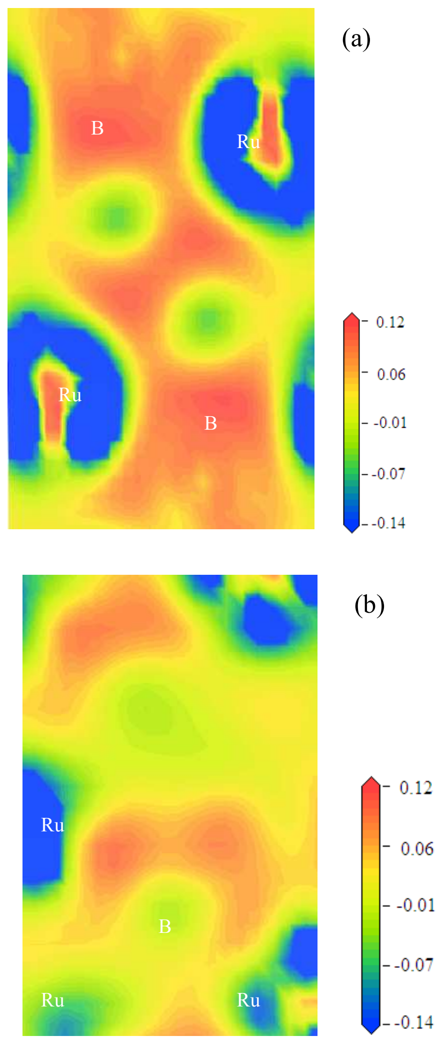

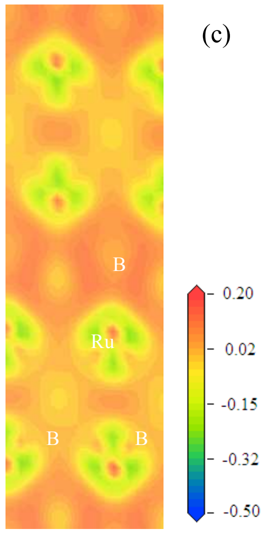

Fig. 3 The difference charge density contour plots of chemical bonds in RuB_{2-x} borides. (a) RuB_2 (110) plane. (b) RuB (110) plane. (c) Ru_2B_3 (010) plane, respectively.

occurs at the weak Ru-B covalent bonds. For RuB, we observe that there is no charge accumulation between B and B atoms. The RuB has only the network Ru-B bond and the network bond states with synergistic effect can enhance the resistance to deformation.

For Ru_2B_3, each Ru atom is surrounded by seven B atoms, and each B atom is surrounded by four Ru atoms. This atomic arrangement can be viewed as the alternatively stacked Ru and B layers along the *c*- direction. Moreover, the B layer is composed of two sub-boundary B layers. Therefore, the staggered B and Ru layers form two types of Ru-B bonds including the Ru-B (1) bonds (2.175 Å) and Ru-B (2) bonds (2.187 Å) and one type of B-B covalent bond (1.804 Å), which is in good agreement with the experimental value[24]. It is interesting to find that the B-B and Ru-B covalent bonds form triangular pyramid bonds in Ru_2B_3, while B-B covalent bond as base and the Ru-B covalent bonds as two sides. Therefore, the B-B and Ru-B covalent bonds in *a-c* plane and the B-B covalent bonds compensate the bonding energy of weak Ru-B covalent, which is origin of the bigger elastic modulus and high hardness.

The calculated electronic density of states (DOS) of RuB_2, RuB and Ru_2B_3 are shown in Fig. 4, in which the black vertical dashed line represents the Fermi level (E_F). It can be seen that there are some bands across the E_F, indicating that these Ru-based borides exhibit metallic behavior. From Fig.4 (a) to Fig.4 (c), the DOS profiles of RuB_2, RuB and Ru_2B_3 are contributed by Ru- 4*d* states and B- 2*p* states, implying that the local hybridization between Ru and B atoms so as to form the strong Ru-B bonds along the *d-p* direction. The feature of covalent interaction between B and Ru atoms is demonstrated by The difference charge density (see Fig. 3).

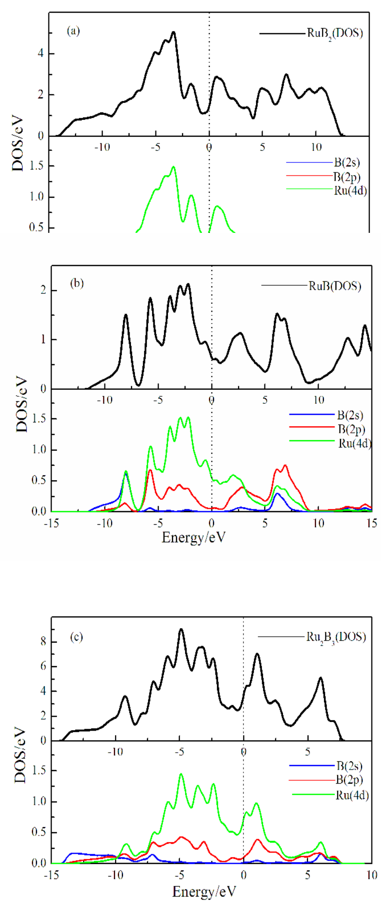

Fig. 4 The total and partial density of states of ruthenium borides. (a) RuB_2. (b) RuB. (c) Ru_2B_3.

As we know, the Ru_2B_3 may be a potential superhard materials, following, the DOS profile of Ru_2B_3 is discussed. From Fig.4 (c), the DOS profile could be mainly divided into three parts. The first part extending from bottom up to -0.57 eV consists mainly of Ru-4*d*, B-2*s* and B-2*p* states, the second from -0.57 eV to 3.58 eV is mainly the contribution of Ru-4*d* and B-2*p* state, and the last part from 3.58 eV to 7.60 eV mainly contains mixtures of Ru-4*d*, B-2*p* and B-2*s* states. The DOS at E_f is controlled by the overlap between the Ru-4*d* and B-2*p* states. Compared with the RuB_2, RuB and Ru_2B_3, the main differences between the PDOS are that the Ru_2B_3 has smooth valley near E_f. This may be because of the Ru-B covalent bonds of the Ru_2B_3 are stronger than those of RuB_2 and RuB. Our calculated results show that the average nearest Ru-B bond length of Ru_2B_3 is shorter than the Ru-B bond lengths within the B-Ru-B of the RuB_2 and RuB structure, and the Mulliken overlap population of Ru-B and B-B covalent bond of Ru_2B_3 are bigger than corresponding bond for RuB_2 and RuB (see table 3 and Fig. 3). There is a reason why the Ru_2B_3 has strong hybridization between B and Ru atoms, and has high hardness.

4. Conclusions

In summary, we have presented first-principles density-functional theory to investigate the structural stability, elastic properties, hardness and electronic structure of RuB_{2-x} ($0 \le x \le 2$) borides. All possible symmetrical configurations with different boron concentrations are discussed in detail. The calculated results show that the formation energies of RuB_{2-x} borides decreased rapidly along the decrease of boron concentration when $x > 0.25$, indicating that the boron-poor region are more stable than that of boron-rich region.

The calculated bulk and shear modulus of Ru_2B_3 are 349 GPa and 202 GPa, respectively, which are bigger than that of RuB_2 and RuB. The Young′s modulus is calculated to be in a sequence of Ru_2B_3>RuB>RuB_2. Obviously, the Ru_2B_3 has a smaller stiffness. The calculated intrinsic hardness of RuB_2 is 36.8 GPa, which is in good agreement with the previous theoretical results. We note that the intrinsic hardness of Ru_2B_3 is about of 49.2 GPa.

The analysis of structural feature and electronic structure show that the high hardness of Ru_2B_3 is derived from the layer structure and bond characteristic. The sub-boundary B and Ru layers form two types of Ru-B and B-B covalent bonds along the *c*- direction, while Ru-B bonds as two sides and B-B covalent bond as base. This triangular pyramid bonds can improve resistance to the shape and shear deformation, and enhance the elastic modulus and hardness. Therefore, we predict that the intrinsic hardness of Ru_2B_3 with hexagonal structure (space group: *P63/mmc*) is about of 49.2 GPa, which is a potential superhard material.

Acknowledgments

Financial support by the National Natural Science Foundation of China (Grant No. 50525204, 50832001 and 50902057) and the important project of Nature Science Foundation of Yunnan (No. 2009CD134) are gratefully acknowledged.

References

1 R. W. Cumberland, M. B. Weinberger, J. J. Gilman, S. M. Clark, S. H. Tolbert, R. B. Kaner, *J. Am. Chem. Soc.,* 2005, **127***,* 7264.

2 Y. Liang, B. Zhang, *Phys. Rev. B*. 2007, **76***,* 132101.

3 A. Latini, J. V. Rau, R. Teghil, A. Generosi, V. R. Alberini, *Appl. Mater. Inter.* 2010, **2***,* 581.

4 J. B. Levine, J. B. Betts, J. D. Garrett, S. Q. Guo, J. T. Eng, A. Migliori, R. B. Kaner, *Acta Mater.,* 2010, **58***,* 1530.

5 A. Knappschneider, C. Litterscheid, D. Dzivenko, J. A. Kurzman, R. Sechadri, *Inorg. Chem.,* 2013, **52***,* 540.

6 Y. Pan, W. T. Zheng, X. Y. Hu, L. Qiao, S. Chen, *J. Alloys. Compd.,* 2014, **587***,* 468.

7 H. Y. Chung, M. B. Weinberger, J. B. Levine, A. Kavner, J. M. Yang, S. H. Tolbert, R. B. Kaner, *Science.* 2007, **316***,* 436.

8 Q. F. Gu, G. Krauss, W. Steurer, *Adv. Mater.,* 2008, **20***,* 3620.

9 S. Chiodo, H. J. Gotsis, N. Russo, E. Sicilia, *Chem. Phys. Lett.,* 2006, **425***,* 311.

10 M. B. Weinberger, J. B. Levine, H. Y. Chung, R. W. Cumberland, H. I. Rasool, J. M. Yang, R. B. Kaner, *Chem. Mater.,* 2009, **21**, 1915.

11 B. J. Suh, X. Zong, Y. Singh, A. Niazi, D. C. Johnston, *Phys. Rev. B.* 2007, **76***,* 144511.

12 A. Šimůnek, *Phys. Rev. B.* 2007, **75**, 172108.

13 Y. Pan, W. M. Guan, W. T. Zheng, *Dalton Trans.* 2014, **43***,* 5168.

14 J. V. Rau, A. Latini, A. Generosi, V. R. Albertini, D. Ferro, R. Teghil, S. M. Barinov, *Acta Mater.,* 2009, **57***,* 673.

15 M. Frotscher, M. Hölzel, B. Albert, *Z. Anorg. Allg. Chem.,* 2010, **636***,* 1783.

16 *MATERIALS STUDIO, Version 4.1, Accelrys In.,* 2006.

17 J. P. Perdew, J. A. Chevary, S. H. Vosko, K. A. Jackson, M. R. Pederson, D. J. Singh, C. Fiolhais, *Phys. Rev. B.* 1992, **46***,* 6671.

18 J. P. Perdew, K. Burke, M. Ernzerhof, *Phys. Rev. Lett.,* 1996, **77***,* 3865.

19 X. F. Hao, Y. H. XU, Z. J. Wu, D. F. ZHou, X. J. Liu, J. Meng, *J. Alloys. Compd.,* 2008, **453***,* 413.

20 R. Hill, *Proc. Phys. Soc. A.* 1952, **65***,* 349.

21 F. Gao, *Phys. Rev. B.* 2006, **73***,* 132104.

22 M. B. Kanoun, I. R. Shein, S. G. Said, *Solid State Commun.,* 2010, **150***,* 1095.

23 P. Yong, Z. Kunhua, G. Weiming, C. Song, *Rare Metal Mat. Eng.,* 2012, **41***,* 2086.

24 M. Frotscher, A. Senyshyn, B. Albert, *Z. Anorg. Allg. Chem.,* 2012, **638***,* 2078.

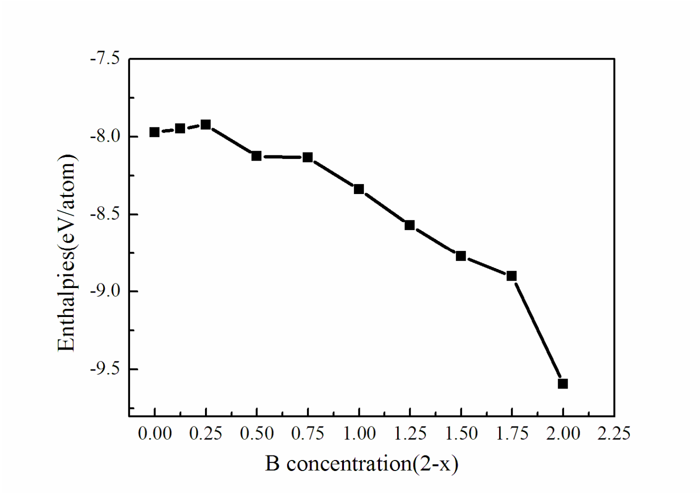

-7.5
-8.0
-8.5
-9.0
-9.5
Enthalpies(eV/atom)
0.00 0.25 0.50 0.75 1.00 1.25 1.50 1.75 2.00 2.25
B concentration(2-x)